

THE TRANSPORT OF MASS, ENERGY, AND
ENTROPY IN CRYOGENIC SUPPORT STRUTS FOR
ENGINEERING DESIGN

Thermal and Fluids Analysis Workshop

August 13-17, 2012, Pasadena, California

J.P. Elchert

NASA Glenn Research Center

Thermal Systems Branch

August 8, 2012

1 Abstract

Engineers working to understand and reduce cryogenic boil-off must solve a variety of transport problems. An important class of nonlinear problems involves the thermal and mechanical design of cryogenic struts. These classic problems are scattered about the literature and typically require too many resources to obtain. So, to save time for practicing engineers, the author presents this essay. Herein, a variety of new, old, and revisited analytical and finite difference solutions of the thermal problem are covered in this essay, along with commentary on approach and assumptions. This includes a few thermal radiation and conduction combined mode solutions with a discussion on insulation, optimum emissivity, and geometrical phenomenon. Solutions to cooling and heat interception problems are also presented, including a discussion of the entropy generation. And the literature on the combined mechanical and thermal design of cryogenic support struts is reviewed with an introduction to the associated numerical methods.

KEYWORDS: Cryogenic • Support • Strut • Heat • Transfer • Cooling • Entropy • Design • Boil • Boil-off • Mass • Transport

Contents

1	Abstract	1
2	Foreword	4
3	Conduction analysis of struts	4
3.1	The basic problem	4
3.2	Materials data pitfalls	5
3.3	Boundary conditions	8
4	Combined mode radiation and conduction with struts	11
4.1	Constant External Emissivity	12
4.2	Extending Boyle and Knoll's Work on Radiation Internal to the Tube	13
4.3	The Critical Length	15
5	Heat interception	16
5.1	Reduced boil off cooling via passive sensible energy	16
5.2	Active cooling via cryocooler	19
5.2.1	Thermodynamics and Minimum Entropy Design	19
5.2.2	Practical cooling scheme to reduce required cryocooler work	23
5.2.3	Commentary on the full mechanical and thermal optimization problem	27

List of Symbols

\dot{q}''	Heat Flux
\dot{q}	Heat Current
\dot{W}	Work
T	Temperature
k	Thermal Conductivity
L	Length

A	Cross sectional area of tube
P	Perimeter of the tube
T	Temperature of tube
h	Heat transfer coefficient
\dot{m}	Mass flow rate
c	Specific heat capacity of fluid
α	Square root of ratio of conduction to convection resistance
β	Number of transfer units
τ	Nondimensional temperature profile
η	Nondimensional length
γ	Defined for reasonable printing of Canavan and Miller's solution
ϕ	Coefficient of Performance
\dot{S}	Entropy Generation
C	Cycle difference factor
\overline{AB}	Segment A to B in schematic
\overline{BC}	Segment B to C in schematic
\overline{DE}	Segment D to E in schematic
\overline{DF}	Segment D to F in schematic
\overline{EF}	Segment E to F in schematic

List of Subscripts

s	Strut
f	Fluid
h	Hot
c	Cold
p	At constant pressure
2	Second stage
rej	Rejection
$Carnot$	Carnot
$Real$	Real
CB	Integrate from C to B in the schematic
BA	Integrate from B to A in the schematic

2 Foreword

This work was supported in part by the Cryogenic Propellant Storage and Transfer project at the NASA Glenn Research Center. I would like to especially thank Robert Christie and William Fabanich for their excellent guidance and advice. Most importantly, this work is dedicated to my best friend and fiancée, Heather, for her invaluable companionship.

3 Conduction analysis of struts

Before delving into the advanced topics, a review of the conduction analysis provides a foundation for this essay. The advanced reader might want to skip to the next section, if so, at least stop and read the commentary on boundary conditions (section 3.3).

3.1 The basic problem

Consider a tube (or rod) experiencing only conduction heat transfer. We know the temperatures at both boundaries, denoted by T_h and T_c . What is the steady state heat flow and temperature profile in the one-dimensional approximation?

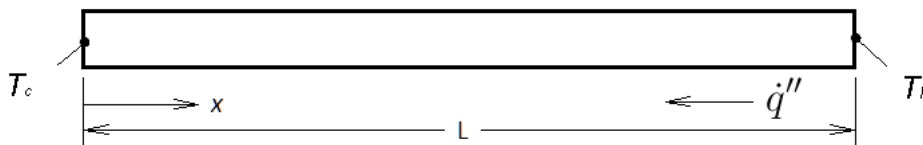


Figure 1: A schematic of a simple cryogenic strut heat leak problem

We will assume steady state, constant cross-section, one-dimensional, no radiation, no convection, and no internal heat generation. The phenomenological law by Fourier may be used to solve for the heat flow and the energy

diffusion equation may be used to solve for the temperature profile.¹

$$\dot{q}'' = -k \frac{dT}{dx} \quad (1)$$

$$\frac{d}{dx} \left(k \frac{dT}{dx} \right) = 0 \quad (2)$$

In general, for cryogenic struts, it is common for the solid to experience large temperature gradients, often from 77K or less up to 250K or more. So the assumption of constant thermal conductivity is a poor choice. When the thermal conductivity becomes temperature dependent, the governing equation no longer has a constant coefficient so the problem becomes nonlinear. In fact, it is much easier to find the heat flow than the overall temperature gradient because separation of variables may be deployed.

$$\int_0^L \dot{q}'' dx = \int_{T_c}^{T_h} -k(T) dT \quad (3)$$

Because the strut is of constant cross-section, this equation simplifies even further.

$$\dot{q}'' = \frac{1}{L} \int_{T_c}^{T_h} -k(T) dT \quad (4)$$

At this point, the challenge is integrating the thermal conductivity. For most materials of interest, the thermal conductivity as a function of temperature is known through testing. Most of these functions may be approximated explicitly with logarithmic or polynomial curve fits. The National Institute of Standards and Technology offers this data for over a dozen materials on their website[17]. They typically give fits using summed powers of logarithms that are okay for numerical integration, but, as we will see, not so great for solving for the temperature profile.

3.2 Materials data pitfalls

I should point out some of the pitfalls associated with curve fits of material data. First, it is possible to create a fit that does not follow the profile of

¹Usually, the energy equation is solved for the temperature profile and the derivative of the temperature profile is used in Fourier's Law to obtain the heat flow. But in this case, because it was steady state, no heat generation, and adiabatic sides, the heat transfer rate is a constant independent of x. This is a consequence of conservation of energy[14]

the function. This is especially true of polynomials. Sometimes a poor fit will veer off in the middle or tail off at the end. In general, always plot the fit to make sure it matches the function. Also, as a general rule, never extrapolate material properties data. Without a complete understanding of the crystalline and grain structure of a material, we cannot trust extrapolating a curve fit (especially a polynomial) beyond the intended domain.

Instead of doing a polynomial fit, an engineer might choose to interpolate the values from a table. If there are too few samples populating the table, essential features of the thermal conductivity curve may be missed. I recommend intervals of 1K to 5K (or smaller), depending on the curvature of the real measured data.

One material on NIST's website is stainless steel 304. Assuming stainless steel 304 is the strut material, $T_h = 200\text{K}$, $T_c = 20\text{K}$, and $L = 1\text{ft}$, the heat flux turns out to be $-0.53 \frac{\text{W}}{\text{cm}^2}$ using the temperature dependent form. However, assuming constant properties evaluated at the arithmetic mean of the prescribed bounds, we find $-0.46 \frac{\text{W}}{\text{cm}^2}$: an underestimate of the true value by a relative error of -13%.

We might also want the temperature profile. Examine the diffusion equation. The temperature dependent thermal conductivity makes the problem nonlinear and separation of variables will not work by itself. Like most differential equations, having foresight is key to being able to solve the problem efficiently. So consider a function that, to the untrained eye, appears unrelated to the problem.

$$\theta(T) \equiv \int_0^T -k(T) dT \tag{5}$$

It follows from the fundamental theorem of calculus that this equation may be written in terms of the derivative instead.

$$\frac{d\theta}{dT} = k(T) \tag{6}$$

Using the chain rule to substitute this expression into equation 2 (or simply using Leibniz notation to cancel differentials) makes the problem solvable. This method is known as 'Kirchhoff's transformation'[15]. So, continuing the solution,

$$\frac{d^2\theta}{dx^2} = 0 \tag{7}$$

The boundary conditions must also be transformed.

$$T(0) = T_c \Rightarrow \theta(T(0)) = \theta(T_c) \quad (8)$$

$$T(L) = T_h \Rightarrow \theta(T(L)) = \theta(T_h) \quad (9)$$

The solution to this equation can be obtained with straightforward integration.

$$\theta(x, T) = \frac{\theta(T_h) - \theta(T_c)}{L}x + \theta(T_c) \quad (10)$$

All that is left is to evaluate θ , which requires integration of the thermal conductivity. The problem is that it can be difficult to integrate the thermal conductivity. Therefore, for this case, I simplified the NIST logarithmic fit by re-fitting the data to a quadratic polynomial.

$$k(T) = a + bT + cT^2 \quad (11)$$

For stainless steel 304, the coefficients (valid only from 20K to 200K) turn out to be $a = 0.899914 \frac{W}{m \cdot K}$, $b = 0.103523 \frac{W}{m \cdot K^2}$, and $c = -0.000222 \frac{W}{m \cdot K^3}$. Be aware that rounding the coefficients will result in massive errors—as a general rule, never truncate intermediate calculations. Checking the curve fit (see Figure 2), notice that it falsely turns downward above 200K and is slightly off the mark near 20K.

Because the functional form of the thermal conductivity is given, we may now write the final solution in terms of T and x . Unfortunately, the equation is implicit and requires iteration to solve.

$$aT + \frac{b}{2}T^2 + \frac{c}{3}T^3 = \frac{\theta(T_h) - \theta(T_c)}{L}x + \theta(T_c) \quad (12)$$

The iteratively solved temperature profile is shown in Figure 3, along with the finite difference solution. In the finite difference solution, the thermal conductivity was not represented by a quadratic polynomial. Instead, actual data from a NIST logarithmic fit was tabulated in 5K intervals and interpolated linearly. It is likely that the finite difference solution is more accurate and the difference seen in the temperature gradient at the cold end has to do with the inaccuracies produced by the quadratic fit of the polynomial.

Thermal conductivity of stainless steel 304

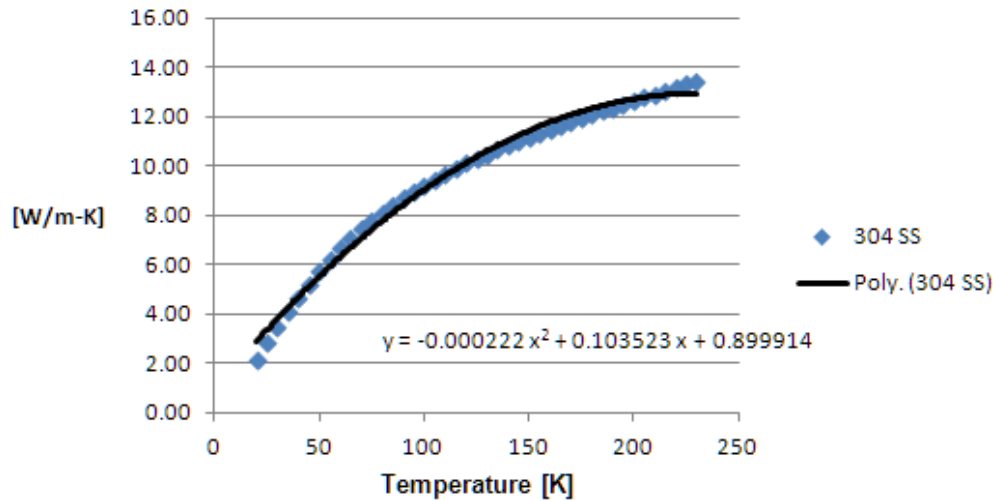


Figure 2: Notice how the quadratic fit does not fit well when extrapolated beyond 200K, even though the fit was created with data from 20K to 230K. Also, notice the mismatch near the left of the plot.

3.3 Boundary conditions

The astute reader will point out that we need more information for an answer representative of the real system. The problem is the hot boundary condition. By assuming a hot temperature, we are indirectly assuming the heat flow; albeit, now it must be solved with an equation and integral. Engineers rarely have a full thermal simulation available when designing supporting structures yet estimating the heat leak is critical to system design.

To shed light on the nature of this boundary condition, consider a different heat transfer problem: the 1967 vapor cooled tube experiment by A.G. Fox and R.G. Scurlock[11]. In their experiment, two identical stainless steel tubes of 12.5 mm diameter and 0.2 mm wall thickness led into the liquid helium container (which was shielded with liquid nitrogen). One tube (upper temperature profile in Figure 4) was closed at the top. The authors remarked,

It was found that when helium vapor flowed up both tubes, the total heat reaching the liquid helium was 0.012W. Under

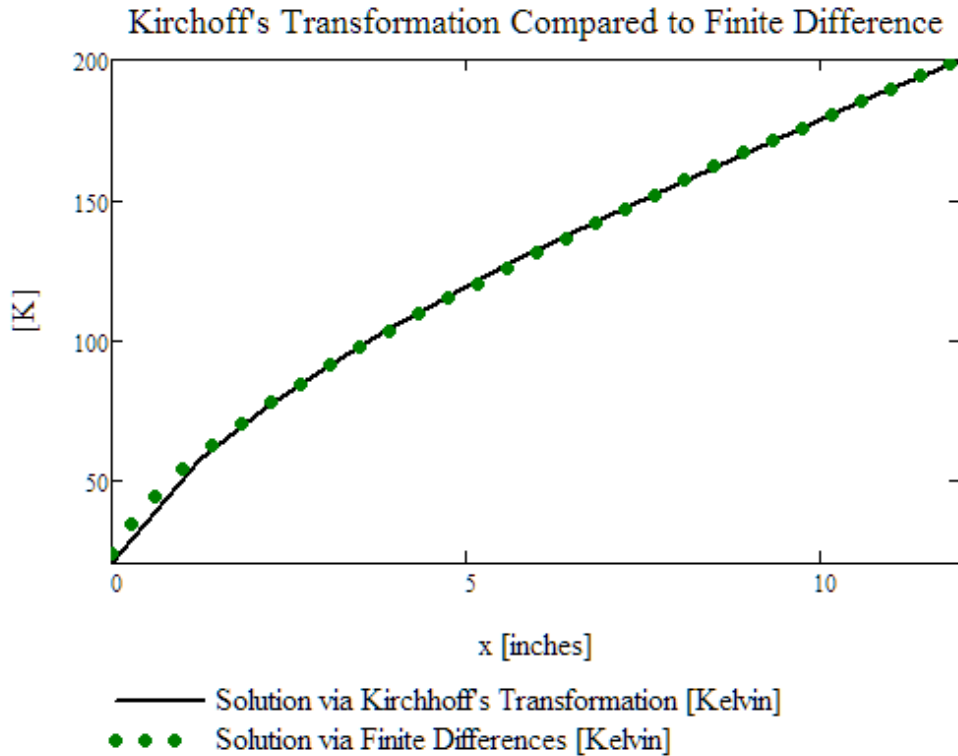


Figure 3: Here, the governing equation was solved both analytically and with finite differences. The analytical solution used a quadratic approximation for the thermal conductivity. The solution with finite differences, on the other hand, interpolated linearly from tabulated thermal conductivity data.

this condition, the calculated heat by [solid] conduction down the open vapor-cooled tubes was less than 0.001W. However, when one tube was closed off at the room temperature end, the total heat was observed to increase to 0.028W: an increase of 0.016W. . . the increase therefore arose almost completely from the conduction through the closed tube walls. . . the temperature profiles in the open and closed tubes were plotted using a copper-constantan thermocouple. These are shown in the figure and demonstrate clearly that the temperature gradient was substantially reduced by vapour-cooling.

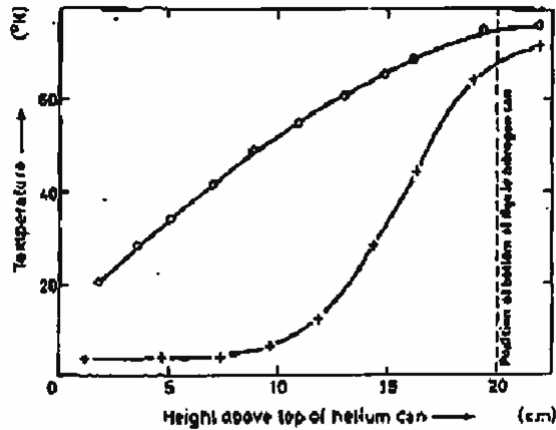


Figure 1. Temperature profiles in open tube + and closed tube O

Figure 4: Fox and Scurlock’s experimental data is depicted here; notice how the hot boundary condition differs between the open and closed tubes (lower and upper plots, respectively). Note that in this experiment, ‘open tube’ means the boil off gas was allowed to flow through the tube. Later, ‘open end’ refers to a tube in a radiation environment so be careful not to confuse the two.

Fox and Scurlock, by trying to point out the benefits of boil off cooling, also demonstrated the way in which the hot boundary condition depends upon external factors². It is inappropriate to assume boundary conditions at parts that are, essentially, in the middle of the thermal network. There is no physical reason to justify this approach because there is no boundary condition at that location. The strut is connected to several thermal pathways before reaching the dominating environmental heat sinks. These pathways coupled with the strut and the tank accurately determine the heat flux.

So far, our approach to estimating the hot boundary condition is, for a ground test, to refer to past experiments or use heaters for hot temperature control. In a ground based application, it is reasonable to assume ambient conditions for the hot boundary temperature. For a spacecraft, on the other hand, people often assume the environmental sink temperature is representative. Really, these techniques are all engineering approximations that serve

²With this view, a more accurate temperature profile would be obtained with a Neumann boundary condition but that requires assuming the heat flow *a priori*.

to get an estimate so other parts of the design may be appropriately sized.

Most of the time, in the literature, the reader will find authors using something like the saturation temperature of the cryogenic fluid at the cold boundary condition, roughly 20K for a representative liquid hydrogen tank temperature. But there exists some mechanical link fastening the strut to the tank and there will be a change in temperature across this interface. This temperature change varies considerably depending on the method of attachment. For an example, see the temperature change across the strut attachment plate³ in Figure 5.

Also, observe the large thermal gradient across the struts in Figure 6. We may conclude that because a large temperature gradient exists across the struts, they must be design to perform well as insulators. Its clear that the cross sectional area must be minimized. This problem may be solved using an optimized combined thermal-structural-vibrations analysis such as a modified version of the classic study⁴ by Bushnell[7]. An introduction to the literature on this approach is given in section 5.2.3.

4 Combined mode radiation and conduction with struts

Energy exchange via thermal radiation is happening all around us, everywhere, all of the time. It's particularly important in space because heat transfer is dominated by the combined modes of conduction and infrared radiation. Herein are a few noteworthy solutions that I hope will provide some insight into your own design problems.

³NASA Glenn Research Center's Cryogenic Propellant Storage and Transfer program funded a reduced boil-off technology (colloquially referred to as 'Broad Area Cooling') demonstration called Cryogenic Boil-off Reduction System in 2012. The prototype was undergoing bake-out at the time of this writing.

⁴To help the reader find this document: submitted February 21 1983; presented as Paper 83-0829 at the AIAA/ASME/ASCE/AHS 24th Structures, Structural Dynamics and Materials Conference, Lake Tahoe, Nevada, May 2-4, 1983; published by AIAA with permission.

4.1 Constant External Emissivity

Consider another stainless steel 304 strut, this time a 1 inch diameter tube with a wall thickness of 0.06 inches and open ends. This strut now exists in a radiation environment. We assume large, isothermal surroundings, gray-diffuse radiation exchange, and neglect the radiation exchange internal to the tube (for now)⁵.

If the surroundings temperature is between the hot and cold conduction boundaries (assume 150K, 300K, and 20K, respectively), a curious phenomenon may occur. By definition, part of the strut will be warming and part of it will be cooling. If the entire strut is coated with the same emissivity⁶, does there exist a value that minimizes the total heat flux? If so, what is that value?⁷

So, to observe trends, the graphical solution was obtained by sweeping across the emissivity domain (see Figure 7). Although not shown in the plot, when solving for a lower surroundings temperature, one may demonstrate that the optimum amount of insulation falls with the surroundings temperature. It becomes better to go more uninsulated in that case. Albeit, the practical usefulness of this solution is typically limited—unless the strut has a view to deep space, the surroundings temperature, defined by the vehicle’s skin, is rarely less than 200K. From this we may draw the inference that, if possible, struts and tanks should be given more view to deep space, although the ability to do this is balanced by other concerns like micrometeorites and orbital debris.

After reading carefully, one might ask, “But aren’t we restricting ourselves by requiring that the entire surface have the same coating optical property? What if we could put a high emissivity paint on the part of the strut warmer

⁵For more information about these assumptions, refer to chapters 12 and 13 of the Fundamentals of Heat and Mass Transfer[14] by Incropera and DeWitt.

⁶I assumed constant emissivity in all of these cases, going against the advice given including the temperature dependence. However, I have been unable to find wavelength dependent emissivity data in the far infrared. Although temperature dependent emissivity values for various metals have been published and may be utilized, at the time of writing, I had not had a chance to implement this strategy via finite differences. Typically, this requires re-calculating radiation conductors so, for folks using SINDA based tools, this requires custom logic. Nevertheless, because the emissivity for most materials decreases with decreasing temperature, using the room temperature value is conservative.

⁷I first saw this problem in CRTECH’s Sinaps User’s Manual, Cryogenic Tank Support tutorial[10].

than the surroundings temperature and just insulate the colder part?” Of course, with enough information about the surroundings and view factors, this is a nice passive technique for further reductions in heat leak. This exercise is left for the reader.

4.2 Extending Boyle and Knoll’s Work on Radiation Internal to the Tube

In November 1968, Robert Boyle and Richard Knoll published a NASA technical note titled, “Thermal analysis of shadow shields and structural members in a vacuum” [6]. Several neat solutions were published, along with the FORTRAN program they used to obtain their results. Essentially, they solve shadow shield problems with an iterative method and strut problems with a finite difference method.

Although they cover a variety of interesting and fundamental problems, we will just focus on their work on the radiation exchange inside a conducting hollow tube. Like me, they also considered a constant internal emissivity, solving for a family of dimensionless heat transfer rate curves. Observe their results in Figure 8. Notice the steep gradient near the lower emissivity values, as well as the dependence on external emissivity.

Boyle and Knoll figured that the increase in heat transfer due to internal radiation may be thought of as having two components:

From these figures, it can be seen that both the internal and external emissivities can affect the heat transfer rate...in these cases, the surroundings were taken to be at zero temperature. Increasing the internal emissivity causes an increase in the heat transfer rate at the colder end of the strut in a twofold manner. First, as the internal emissivity increases, the temperatures along the strut increase. This increases the thermal gradient at the colder end which results in an increased conducted heat heat transfer rate. Second, for closed ends, increasing the internal emissivity increases the amount of radiant energy which is absorbed by the end of the strut.

In other words, some of the increased heating is due to the sidewalls and some is due to the irradiation of the hot closed end and the absorption at cold closed end. Boyle and Knoll do not discuss the relative magnitude of

these two effects. But using axial shielding is a common practice (see Figure 9 for a depiction) so it is important to understand how much benefit we get from the added complication of installing these shields⁸. So is it better to insulate the sidewalls in the radial direction, perhaps with a rolled tube of multilayer insulation? Or should one try to insulate the axial view, maybe using discs spaced along the length of the strut? Or is some combination of the two optimal?

I have answered that question for the case of a closed end, 12 inch stainless steel 304 tube that is 1 inch in diameter and has a 0.06 inch wall thickness (see Figure 10 for the solution and Figure 9 for a depiction of the finite difference and Monte Carlo thermal model). The hot, cold, and surroundings temperatures were 300K, 20K, and 200K, and the internal emissivity (emissivity of the inner wall of the tube, possibly under a blanket in some cases) was swept from 0 to 1. The discs, or ‘shields’, if used, were coated with a specified emissivity on both sides, assumed to have zero thickness and zero heat capacity (arithmetic, or instant response, surfaces⁹), and were always spaced equally.

Most importantly, the scale of these results show that for representative struts, the internal radiation only increases the heat transfer by about 1%¹⁰ when compared to the solution neglecting this effect. Now, we will examine the results in detail.

Starting at the top of the legend in Figure 10, the blue diamonds depict re-radiating ends. This simulates perfectly insulated surfaces that do not allow for radiation emission. Instead, they just reflect and absorb. Once they are allowed to emit, like in the second series (red squares) notice how the heat transfer rate increases. This suggests that the hot and cold ends’ views to each other and the sidewall is important in this problem¹¹. Now, when I add one disc of emissivity 0.28 to the middle of the strut, the heat

⁸If the shields are easy enough to install, this might not be much of a concern. So if the reader has that opinion, then these results are just for general knowledge, because said reader is going to use shielding anyways.

⁹This results in a faster run time for the steady state case but the validity of this approach should be checked for a transient solution.

¹⁰In composite tubes, the decreased thermal conductivity makes radiation heat transfer a little more important. So for composites, an increase in heat transfer rate of 5% is typical. Obviously, the precise results for different materials and geometries needs to be evaluated on a case by case basis taking into account the length to diameter ratio.

¹¹By the way, only series 4, 7, 8, 9, 10, and 11 had exterior blankets. The rest of the cases assumed no exterior blanket.

leak actually gets worse (series 3, green triangles). It's not much better if the shield is 0.04 emissivity (series 5, blue lined 'x') and both one shield cases are worse than no shield at all. Now, examine the solution with multilayer insulation on the outside of the tube.

By leaving the single 0.04 emissivity shield in place and blanketing the exterior with a typical blanket of effective emissivity 0.01, we find the curve translates down significantly (series 4, violet 'x'). So, for these boundary conditions, the external surface blanket is very important¹².

Getting rid of both the external blanket and the shield and instead insulating the sidewall (series 6, filled orange circle) with a typical blanket (effective emissivity 0.01) results in somewhat worse performance, as expected due to the removal of the *exterior* blanket.

Both the exterior and interior surfaces were blanketed in series 7 and no shields were used (blue plus sign). Surprisingly, this one performs much like the case with 7 shields but no blankets at all (series 12, orange triangles). Another interesting fact is that it doesn't appear to matter how well the shields contact the tube (see series 9 and 10).

Obviously, the best case was series 13 (gray box with blue cross). Over the entire domain, insulated sidewalls and seven radiation shields effectively eliminate this small mode of heat leak.

4.3 The Critical Length

It turns out that when the large, isothermal surroundings temperature is between the hot and cold boundary temperatures (such as 220K, 300K, and 20K, respectively), there is a critical length such that no matter how much longer the tube is, the heat leak will not change. To see why, consider the temperature profile solution (Figure 11) of two struts of the same emissivity, only differing in length.

Observe the gradient near the cold side. Both curves end up having very similar gradients such that the heat flux is negligibly different between these two geometries, even though one is over twice as long. This happens because the 'warm' section tries to equilibrate to 220K in both cases—more so in the 100 inch case—and if the tube is long enough, the 'middle' section will end up at steady state with the surroundings.

¹²This dovetails with what we already know. Recall? In the previous section, we found that for the 300K hot case with a 200K surroundings temperature, the optimal external emissivity is 0.

To find this critical length, consider an infinitely long rod in some large, isothermal surroundings at some temperature of interest (in my example 220K) with a base temperature at the temperature of the cold sink (usually close to a cryogenic fluid’s temperature) and solve for the location on the tube where the temperature is some number very close to the surroundings temperature, say within a fraction of 0.99. This is essentially the radiation fin problem.

Readers interested in solving this problem will be able to adapt one of A.R. Shouman’s excellent solutions[18] in “Nonlinear heat transfer and temperature distribution through fins and electric filaments of arbitrary geometry with temperature-dependent properties and heat generation”. Shouman also provides a list of references of authors with the same solution but different mathematical formulations.

5 Heat interception

The utility of sensible cryogenic heat interception via boil off gas was recognized many years ago. Further reductions in boil off rates require active cooling. But as the operating temperature falls so does the coefficient of performance. Since current technology requires significant size and input power for adequate cooling capacity, maximizing the efficiency of the various cooling schemes is paramount. And of equal importance is the concept of heat interception, which reduces input power by picking up some heat at warmer stages. In this section, these topics are discussed in detail.

5.1 Reduced boil off cooling via passive sensible energy

A cryogenic fluid is vented as it vaporizes. Like Fox and Scurlock[11] showed many years ago, this gas may be used to intercept heat. If flowed concurrently with the struts, the sensible energy of the gas stream increases as it pulls heat away from the strut, transporting it to the vent where it is jettisoned. A diagram of this system is shown in Figure 12.

Think about this problem for a moment. The radiation boundary condition will necessitate blanketing on the outer cylinder. Expanding our thoughts further, the pragmatic engineer would likely replace this concentric tube configuration with a coil¹³. Some folks use a single vent line, wrapping

¹³There certainly exists optimum coil geometry for this case but I have neither attempted

it around the system from strut to strut, coiling it for just a few turns at discrete locations on each successive strut. Others might run a single line for each strut, resulting in multiple vent holes. On the other hand, as opposed to tubular struts, I have seen at least one reference to a design starting with a solid rod and flowing the gas through an array of holes bored axially through the solid, unifying and co-locating the strut attachment and the vent holes.

To press onward, we must settle with simplifications. The one-dimensional concentric tube configuration is straightforward compared to a helical tube analysis so that is a good place to start. The strut is considered to be well insulated from the surroundings and the geometry should be known from a structural optimization analysis¹⁴.

Obviously the result of the energy balance and Taylor expansion (neglecting higher order terms) is two coupled first order ordinary differential equations with variable coefficients:

$$\frac{d}{dx} \left(kA \frac{dT_s}{dx} \right) - hP(T_s - T_f) = 0 \quad (13)$$

$$\dot{m}c_p \frac{dT_f}{dx} - hP(T_s - T_f) = 0 \quad (14)$$

Here, the thermal conductivity of the solid and the specific heat are functions of temperature. The heat transfer coefficient is likely laminar and possibly in the entrance flow regime for some of the vent length. Chi K. Tsao, carrying out research at the Naval Ship Research and Development Center, solved this problem numerically in his well written paper titled, “Temperature distribution and power loss of a gas-cooled support for a cryogenic container” [19] with the restrictions of constant cross sectional area and constant, fully developed heat transfer coefficient.

The cross sectional area could be a function of ‘x’¹⁵, if researchers found a variable cross section to be optimal. For the sake of simplicity, assume the thermo-physical properties, the cross sectional area, and the heat transfer coefficient are all constant. Then this permits an analytical solution of the

nor found this solution. I would be surprised, though, if this problem has not already been solved.

¹⁴I am not aware of a detailed combined boil off line and strut coupled thermo-mechanical optimization solution. In my experience, engineers have been able to optimize the strut via structural analysis, sizing the thermal system based on that design.

¹⁵Interestingly, Tsao considers the cross sectional area to be a function of temperature, making passing mention of that idea in the introduction of his aforementioned paper.

two temperature profiles and the heat current as a function of mass flow rate¹⁶.

E. R. Canavan and F. K. Miller published[8] this solution in 2007 for the Joint Cryogenic Engineering Conference for the case of $T_c = 0$. Building off their work, I was able to extend the solution to all cold temperatures using a simple and well known transform. To complete this analysis, first, nondimensionalize all of the unknowns.

$$\eta = x/L \quad (15)$$

$$\tau_f = \frac{(T_f - T_c)}{(T_h - T_c)} \quad (16)$$

$$\tau_s = \frac{(T_s - T_c)}{(T_h - T_c)} \quad (17)$$

$$\beta = \frac{hPL}{\dot{m}c_p} \quad (18)$$

$$\alpha = \left(\frac{L/(kA)}{1/(hPL)} \right)^{1/2} \quad (19)$$

The Dirichlet boundary conditions are given and transformed in the following three equations.

$$T_s(x = 0) = T_c \Rightarrow \tau_s(\eta = 0) = \frac{T_s(x = 0) - T_c}{T_h - T_c} \quad (20)$$

$$T_s(x = L) = T_h \Rightarrow \tau_s(\eta = 1) = \frac{T_s(x = L) - T_c}{T_h - T_c} \quad (21)$$

$$T_f(x = 0) = T_c \Rightarrow \tau_f(\eta = 0) = \frac{T_f(x = 0) - T_c}{T_h - T_c} \quad (22)$$

With some clever substitutions, transformations, and the assumption of constant properties, the general equations may be written as follows:

$$\frac{d^2\tau_s}{d\eta^2} = \alpha^2(\tau_s - \tau_f) \quad (23)$$

¹⁶Because the solution is simply a function of mass flow rate, it is general and can be extended to pumped loops.

$$\frac{d\tau_f}{d\eta} = \beta(\tau_s - \tau_f) \quad (24)$$

This is the same system of equations solved by Canavan and Miller, demonstrating how relaxing the restriction on the cold boundary condition does not change the result significantly. For the reader's convenience, Canavan and Miller's extended solution is shown in equation 26, with the vast majority of the credit belonging to them[8]. Note that in this formulation, the arbitrary introduction of γ is motivated primarily for readability.

$$\gamma^2 = 4\alpha^2 + \beta^2 \quad (25)$$

$$\frac{\dot{q}''}{k(T_h - T_c)/L} = \left. \frac{d\tau_s}{d\eta} \right|_{\eta \rightarrow 0} = \frac{\gamma(\gamma^2 - \beta^2)}{(\gamma + \beta)^2 e^{\frac{\gamma - \beta}{2}} - 4\gamma\beta + (\gamma - \beta)^2 e^{-\frac{\gamma + \beta}{2}}} \quad (26)$$

It's not obvious at first glance but this solution is only dependent on mass flow rate¹⁷. With that in mind, it's relatively simple to extend the solution to the boil-off rate problem for a single strut. Because the heat leak is approximately equal to the product of the mass flow rate and the latent heat of vaporization of the cryogenic fluid, equating those quantities and solving iteratively results in simultaneous solution of the passively reduced heat leak and the mass flow rate.

For more information, read Canavan and Miller's publication[8] in full. It's a worthwhile read because they go on to discuss how to analytically ballpark tube scaling with tank size as well as the numerical solution of a helical tube bonded to a thin, squat cylindrical support.

5.2 Active cooling via cryocooler

5.2.1 Thermodynamics and Minimum Entropy Design

Imagine a strut being cooled continuously at each point by a different infinitesimal refrigeration cycle. In fact, each differential cooler could be considered a separate Carnot cycle. On the one hand, the coefficient of performance decreases with decreasing temperature, favoring cooling on the warm

¹⁷To check this solution, set the mass flow rate equal to zero and see if the result matches the solution for simple, constant properties conduction through the solid.

side. But with prescribed boundary conditions, the effect of removing heat at warmer temperatures is to increase the temperature gradient at the warm end and decrease the temperature gradient at the cold end (see Figure 15). In other words, the more heat removed close to the hot boundary, the more heat that is pulled into the strut. With a little thought about these two conflicting goals (see Figure 13), it becomes obvious that there exists a distribution of heat removal which results in the minimum cycle input work.

A number of assumptions are required to derive the solution to this problem. The cooling is provided by a continuous distribution of differential, ideal, reversible Carnot cycles. Keeping in mind the spirit of the ideal solution, also neglect the constriction effects of shape factor and contact resistance between the coolers and the strut. In summary, the conduction through the strut is the only irreversible process being considered. Going further, it is logical to assume constant area to length ratio and constant thermal conductivity¹⁸ for the most basic analysis. One last simplification: the hot boundary temperature equals the heat rejection temperature (this may not always be true, especially in space applications).

The solution was, to my knowledge, first published by Adrian Bejan¹⁹ in his 1975 doctoral thesis titled, “Improved thermal design of the cryogenic cooling system for a superconducting synchronous generator”. On page 31, Bejan notes that this problem is simplified if the entropy balance is considered instead of the energy balance. This is a crucial observation that deserves a historical perspective so, please, allow me to expand the discussion for a moment.

It is entirely possible that this idea led to his research into, what he has coined, the constructal law of nature. For our problem, the equivalence between the minimum work and minimum entropy generating configurations is just a special case of the constructal law which posits that for a finite sized system (like a species, a tree, or a river bank) to continue to persist through

¹⁸Bejan solves the temperature dependent formulation of this problem numerically[3].

¹⁹Adrian Bejan, J.A. Jones Professor of the Duke Department of Mechanical Engineering and Materials Science, is ranked among the 100 most highly cited authors worldwide in engineering (all fields, all countries), a recipient of 16 honorary doctorates from universities in 11 countries, and the author of 25 books and 530 peer-referred articles. He has contributed significantly to the fields of thermodynamics, heat transfer, fluid mechanics, convection, and porous media. He is credited with formulating the constructal law of nature and has his own dimensionless number (the Bejan number, Be , is the ratio of heat transfer irreversibility to total irreversibility due to both heat transfer and fluid friction).

time, it must evolve such that, over time, it develops progressively easier access to the imposed current[5]. This is widely considered a unifying law. The best description is in his own words[5]:

The constructal law is the statement proclaiming the existence and the time direction of the evolution of configuration. It is far more general than ‘maximum entropy production’. It is not a statement of optimality (min, max), end design or destiny. No flow system is destined to end up in a certain configuration at long times.

This formulation casts a wide net, covering both entropy generation minimization in biology and engineering and entropy generation maximization in geophysics; from the minimization of flow resistance (rivers) or the maximization of flow resistance (animal fur), to the origin of turbulence (maximization of growth rate of flow deformations) to the homogeneous distribution of stress in bones. In its most general form, this law includes time and provides a formal framework for understanding the genesis of design in nature[5].

With that historical perspective, Bejan’s classical solution to the cryogenic strut minimum work is presented here to bring awareness to the usefulness of the exergy analysis. From first principles, Bejan shows that the total rate of entropy generated by heat conduction between the two prescribed boundaries is,

$$\dot{S} = \int_{T_c}^{T_h} \frac{\dot{q}}{T^2} dT \quad (27)$$

This is a special case of the Gouy-Stodola theorem, which is the balance between lost available energy (exergy) and the irreversible generation of entropy. Bejan’s insight was that non-optimal refrigeration temperatures and locations would naturally result in more entropy generation. If the problem could be formulated in terms of entropy, then the generation of entropy could possibly be minimized. And, of course, he was correct.

A constraint on this problem is that the strut geometry must remain unchanged throughout the optimization process. Presumably, the finite size, semi-unconstrained optimization problem is more in line with the modern formulation of the constructal law. But that is a much more difficult problem and will not be studied here. With that said, this geometrical constraint may be expressed as a constant: the area to length ratio (equation 28),

$$\int_0^L \frac{1}{A(x)} dx = \frac{L}{A} \quad (28)$$

And from substituting for dx using Fourier's Law,

$$\frac{L}{A} = \int_{T_c}^{T_h} \frac{k}{\dot{q}} dT \quad (29)$$

Now, the problem reduces to finding the function $q(T)$ which minimizes equation 27 while satisfying the geometrical constraint in equation 28. The entropy minimizing heat removal solution²⁰ to the variational calculus problem is,

$$\dot{q}_{optimum} = T \left(\frac{\lambda k}{T_h} \right)^{1/2} = T \sqrt{k} \left(\frac{A}{L} \right) \left(\int_{T_c}^{T_h} \frac{\sqrt{k}}{T} dT \right) = \frac{kA}{L} \ln \left(\frac{T_h}{T_c} \right) T \quad (30)$$

where λ is the Lagrange multiplier. In the temperature dependent formulation, λ equals,

$$\lambda = T_h \left(\frac{A}{L} \right)^2 \left(\int_{T_c}^{T_h} \frac{\sqrt{k}}{T} dT \right)^2 \quad (31)$$

and the corresponding minimum generation of entropy,

$$\dot{S} = \frac{A}{L} \left(\int_{T_c}^{T_h} \frac{\sqrt{k}}{T} dT \right)^2 = \frac{kA}{L} \left[\ln \left(\frac{T_h}{T_c} \right) \right]^2 \quad (32)$$

The solution is in terms of temperature and implicitly x ²¹. Note the proportionality to the temperature. The amount of heat removed is proportionately increasing with x , confirming the initial conjecture that it is more efficient to remove bigger chunks of heat at the warmer temperatures.

Extending Bejan's solution, M.A. Hilal and R.W. Boom showed[12] that for the reversible case, as the number of intercepts increases to infinity, the required Carnot cycle work is

²⁰For readers interested in the full variational calculus problem, M.A. Hilal and R.W. Boom give a nice summary in their 1977 paper, "Optimization of mechanical supports for large superconductive magnets"[12].

²¹Bejan never solves for the temperature profile and neither does Hilal and Boom. As far as I know, that is an open problem.

$$\dot{W} = T_h \int_{T_c}^{T_h} \frac{\dot{q}}{T^2} dT \quad (33)$$

which, via transitive property with equations 27 and 32, reduces to the following form:

$$\dot{W} = \frac{A}{L} T_h \left(\int_{T_c}^{T_h} \frac{\sqrt{k}}{T} dT \right)^2 = T_h \frac{kA}{L} \left[\ln \left(\frac{T_h}{T_c} \right) \right]^2 \quad (34)$$

This equation may be used as a baseline for comparison since it represents the ideal, theoretical minimum refrigeration power. Of course, there are more irreversibilities in a real system making this solution the theoretical lowest bound.

5.2.2 Practical cooling scheme to reduce required cryocooler work

In reality, pragmatism grounds the design. It's impossible to physically create a continuous system of differential coolers. While Bejan showed continuous cooling is most efficient, for most applications, it's more practical to cool struts at discrete locations. And although Bejan has shown entropy minimization to be a powerful tool in this analysis, minimization utilizing the energy balance is straightforward for the simplified, discrete, multiple stage problem.

This problem has been solved by numerous authors using a variety of approaches²². Besides Bejan, a few notable authors include Abramson, Hilal, Chato, Khodadidi, and Smith. Bejan first worked on this problem with J.L. Smith, Jr., publishing an article[4] preceding Bejan's 1975 thesis. Hilal and Boom[12] used a gradient based optimizer, Hilal and Eyssa[13] allowed for variable cross sectional area, Chato and Khodadidi[9] minimize entropy by postulating an effective thermal conductivity, and Augusto et al. solve the energy equation analytically for a few special cases[2].

For a sizing calculation, the most expedient method is Hilal and Boom's because gradient based optimizers are so widely available, coming standard with scientific computing packages like Mathematica, MATLAB, MathCAD, and even Excel with the 'Solver' add-in. The basic idea is to set up the energy balances and thermodynamic relationships then search the domain for the

²²In fact, conceptually, it is the same problem as optimizing the location of an intercept in multilayer insulation, only with different heat flow equations.

minimum power solution under a set of constraints assuming each refrigerator is a separate thermodynamic cycle (this assumption may be relaxed if more information about the cycle is known).

This time, consider a constant cross sectional area stainless steel 304 tube 100 cm long. Taking advantage of the full interpolation capability of NIST's fit for stainless steel 304's thermal conductivity, assume the strut's cold prescribed temperature is 4.2K and its hot prescribed temperature is 300K. The tube²³ is being cooled in two locations: one stage at the low temperature end and the other stage at some intermediate temperature at some location on the strut (see the lower drawing in Figure 14 for the schematic).

After specifying the boundary conditions and geometry of the problem, the next step is to define the coefficient of performance, ϕ . It is well known that in general, ϕ is a function of rejection temperature, T_{rej} , but most authors have drawn no distinction between hot prescribed conduction boundary temperature and the cycle's rejection temperature. Often, without saying, they assume that $T_h = T_{rej}$. This is not much of a problem for ground based superconducting magnets—the topic studied by those authors—because on the ground, typically $T_{ambient} = T_h = T_{rej}$. But in spaceflight, the radiator often runs at a higher temperature than the vehicle skin so this distinction becomes important. Even with that in mind, for the purposes of this example calculation, I assumed $T_h = T_{rej}$. Note that, mathematically, the Carnot cycle assumption equilibrates the real and Carnot coefficients of performance.

$$\phi_{Carnot,c} = \frac{T_c}{T_{rej} - T_c} \equiv \phi_{Real,c} \quad (35)$$

$$\phi_{Carnot,2}(T_2) = \frac{T_2}{T_{rej} - T_2} \equiv \phi_{Real,2}(T_2) \quad (36)$$

Many authors define the cycle difference factor, C . This is not necessary because the expression that shows up later on, $C(T) \left(\frac{T_{rej}}{T} - 1 \right)$, could just be represented with the real coefficient of performance: $C(T) \left(\frac{T_{rej}}{T} - 1 \right) = \frac{1}{\phi_{Real}}$. Nevertheless, authors writing in Hilal's tradition have used this form.

$$C_c = \frac{\phi_{Carnot,c}}{\phi_{Real,c}} \quad C_2(T_2) = \frac{\phi_{Carnot,2}(T_2)}{\phi_{Real,2}} \quad (37)$$

²³I used the same assumptions Bejan used for this problem, including perfect heat transfer at a point. Because the discontinuity is inherently neglected, I chose a gradient based approach. In Figure 15, some example temperature profiles are shown.

The energy balances must now be developed so the work may be calculated. Equation 38 defines the first design variable, $\eta_{\overline{AB}}$ (note that $\eta_{\overline{BC}}$ is just derived from $\eta_{\overline{AB}}$ and is simply used for intermediate calculations). Alternatively, one may formulate the segment length AB as the design variable, but using $\eta_{\overline{AB}}$ is in the tradition of Hilal and a start towards full nondimensionalization. Obviously, the other design variable is T_2 .

$$\eta_{\overline{AB}} = \frac{\overline{AB}}{L} \quad \text{and} \quad \eta_{\overline{BC}} = \frac{\overline{BC}}{L} = L(1 - \eta_{\overline{AB}}) \quad (38)$$

With this relationship defined, the temperature dependent heat current equations from C to B and from B to A are defined in the following manner:

$$\dot{q}_{BA}(T_2, \eta_{\overline{AB}}) = \frac{A}{\overline{AB}} \int_{T_2}^{T_c} -k(T) dT \quad (39)$$

$$\dot{q}_{CB}(T_2, \eta_{\overline{AB}}) = \frac{A}{\overline{BC}} \int_{T_h}^{T_2} -k(T) dT \quad (40)$$

Clearly, the work done by the cold stage is defined by,

$$\dot{W}_c(T_2, \eta_{\overline{AB}}) = \left[C_c(T_2) \left(\frac{T_{rej}}{T_c} - 1 \right) \right] (\dot{q}_{BA}(T_2, \eta_{\overline{AB}})) \quad (41)$$

and the difference between equation 39 and equation 40 is equivalent to the heat picked up by the intercept, thus, the intercept's work is defined as,

$$\dot{W}_2(T_2, \eta_{\overline{AB}}) = \left[C_2(T_2) \left(\frac{T_{rej}}{T_2} - 1 \right) \right] (\dot{q}_{CB}(T_2, \eta_{\overline{AB}}) - \dot{q}_{BA}(T_2, \eta_{\overline{AB}})) \quad (42)$$

Finally, the objective function is fully defined and shown in equation 43.

$$\dot{W}(T_2, \eta_{\overline{AB}}) = \dot{W}_c(T_2, \eta_{\overline{AB}}) + \dot{W}_2(T_2, \eta_{\overline{AB}}) \quad (43)$$

Besides the constant geometry, this optimization is subject to a few other constraints. The constraints on the design variables are easy to understand (equation 44 and equation 45), however, equation 46—as obvious as it looks—is easier to forget. Recall Figure 15 and the left most temperature profile. Under certain conditions, its possible for the intercept stage to actually warm the coldest stage, resulting in negative work. That situation is to be disallowed.

Table 1: Solutions to the two stage and three stage example optimization problem

Number of Stages	T_c (K)	T_2 (K)	T_3 (K)	$\eta_{\overline{AB}}$	$\eta_{\overline{DE}}$	$\eta_{\overline{DF}}$
2	4.2	40.0	-	0.351	-	-
3	4.2	21.1	80.7	-	0.194	0.524

$$0 < \eta_{\overline{AB}} < 1 \quad (44)$$

$$T_c < T_2 < T_h \quad (45)$$

$$\dot{W}_c > 0 \quad \text{and} \quad \dot{W}_2 > 0 \quad (46)$$

This solution is easily extended to more stages. Besides adding a cycle and another strut heat transfer segment, additional constraints must be placed on the solution:

$$0 < \eta_{\overline{DE}} < \eta_{\overline{EF}} < 1 \quad (47)$$

$$T_c < T_2 < T_3 < T_h \quad (48)$$

$$\dot{W}_c > 0 \quad \text{and} \quad \dot{W}_2 > 0 \quad \text{and} \quad \dot{W}_3 > 0 \quad (49)$$

In Table 1, the solution to this example problem is shown. Compare this result with Hilal and Boom's in Figure 16. After grappling with a couple nomenclature differences and a typographical error in Hilal and Boom's table (this is described in the Figure 16's caption), it's plain that the solutions match²⁴.

One notable special case of this problem is a cryocooler with a fixed operating temperature. For the same problem, if the intercept temperature was fixed instead to, say, 80K, the relative increase in power was only 25%

²⁴The slight difference may be explained by variations in thermal conductivity approximations, but, because Hilal and Boom never discuss their source of data, this assertion cannot be verified.

even though it was running at twice the optimum temperature. Here, the optimal location was found to be $\eta_{\overline{AB}} = 0.642$. This effect can be understood by observing Figure 17; the ‘hull’ shape of the surface leaves a locus of roughly equivalently performing combinations. In short, every fixed temperature has a unique optimal location, many of which perform similarly.

5.2.3 Commentary on the full mechanical and thermal optimization problem

Throughout this discussion, we have focused on the heat, mass, and entropy transfer aspects of these problems. In all of the example problems, the strut geometry is taken as known. In reality, the strut geometry is driven primarily by the requirement to survive the launch vibrations environment.

In the early 1980s, David Bushnell published[7] the classic solution to this vibrations problem. Relevant, but unrelated to structural analysis, in 2001, Kokkolaras et al. extended Hilal and Boom’s work by using mixed variable optimization to allow for different materials in the strut[16]. Then, in 2002, Mark A. Abramson synthesized[1] those two analysis (even allowing for a variable cross sectional area), but solved the static load case rather than the vibrations case. His semi-unconstrained geometry, combined thermodynamics, heat transfer, mixed material, and load-bearing solution is the current state of the art for ground based systems, obtaining 50% less normalized power[1] than the original design found by Hilal and Eyssa[13].

Still, there are advancements to be made. Abramson’s analysis needs modification for vibrations and geometrical constraints—a full synthesis of Bushnell’s work. Going further, including the shape factor, two dimensional conduction, and the rest of the heat exchanger design would be a huge step forward. Even with these significant increases in difficulty, we would still be neglecting the multilayer insulation and environmental irradiation. It’s exciting that after all these years—even after the groundbreaking work of Bejan, Hilal, Bushnell, and Abramson—there remains unsolved problems in this area of cryogenic engineering.

List of Tables

1	Solutions to the two stage and three stage example optimization problem	26
---	---	----

List of Figures

1	A schematic of a simple cryogenic strut heat leak problem . . .	4
2	Curve fitting the thermal conductivity of stainless steel 304 . . .	8
3	Analytical and finite difference solution of the simple strut. . .	9
4	Heat leak reduction and boundary conditions (Fox and Scurlock)	10
5	Temperature change across strut attachment plate	31
6	Temperature change across struts	32
7	Optimum External Emissivity	33
8	The effect of internal emissivity on heat transfer in cylindrical geometries	34
9	Cutaway of strut thermal simulation	35
10	Solutions to hypothetical configurations as a function of internal emissivity	36
11	Radiation length effect	37
12	Schematic of concentric tubes with the boil off stream in the annulus	38
13	Infinitesimal refrigeration cycles continually cooling	39
14	Schematic of discrete, two stage and three stage cooling	40
15	Example temperature profiles for discrete, two stage cooling .	41
16	Partial view of Hilal and Boom's original table	42
17	Graphical solution of the two stage, discrete optimization problem	43

References

- [1] Mark A. Abramson. Mixed variable optimization of a load-bearing thermal insulation system using a filter pattern search algorithm. *Optim. Eng.*, 5 (2):157–177, 2002.
- [2] Paulo A. Augusto, Teresa Castelo-Grande, Pedro Augusto, and Domingos Barbosa. Optimization of refrigerated shields using multilayer thermal insulation: Cryostats design - analytical solution. *Cryogenics*, Jun 2006.
- [3] Adrian Bejan. *Improved thermal design of the cryogenic cooling system for a superconducting synchronous generator*. PhD thesis, Massachusetts Institute of Technology, Dec. 1974, handwritten edit ‘i.e. Feb. 1975’.

- [4] Adrian Bejan and J.L. Smith Jr. Thermodynamic optimisation of mechanical supports for cryogenic apparatus. *Cryogenics*, pages 158–163, 1974.
- [5] Adrian Bejan and Sylvie Lorente. The constructal law of design and evolution in nature. *Philosophical Transactions of The Royal Society*, pages 1335–1347, 2010.
- [6] Robert J. Boyle and Richard H. Knoll. Thermal analysis of shadow shields and structural members in a vacuum. Technical Note D-4876, NASA Lewis Research Center, Nov 1968.
- [7] David Bushnell. Optimum design of dewar supports. *J. Spacecraft*, 22(4):432–441, 1985.
- [8] E. R. Canavan and F. K. Miller. Optimized heat interception for cryogen tank support. In *Advances in Cryogenic Engineering*, volume 53A and 53B, 2007.
- [9] J.C. Chato and J.M. Khodadidi. Optimization of cooled shields in insulations. *ASME Transactions, Journal of Heat Transfer*, 106 (4):871–875, 1984.
- [10] Cullimore and Ring, editors. *Sinaps User’s Manual*. Cullimore and Ring Technologies, Inc., 2011.
- [11] A.G. Fox and R.G. Scurlock. A letter to the editor. *Cryogenics*, Feb 1967. Department of Physics, University of Southampton, U.K.
- [12] M.A. Hilal and R.W. Boom. Optimization of mechanical supports for large superconductive magnets. In *Proceedings, International Cryogenic Materials Conference in Kingston, Ontario, Canada, 1975*, volume A77-42172 19-31, 1977.
- [13] M.A. Hilal and Y.M. Eyssa. Minimization of refrigeration power for large cryogenic systems. *Advances in Cryogenic Engineering*, 25, 1980.
- [14] Bergman Lavine Incropera, DeWitt. *Fundamentals of Heat and Mass Transfer*. Wiley, 6 edition, 2007.
- [15] Latif M. Jiji. *Heat Conduction*. Springer-Verlag Berlin Heidelberg, third edition, 2009. Founding Editor L.L. Faulkner.

- [16] Michael Kokkolaras, Charles Audet, and Jr. J.E. Dennis. Mixed variable optimization of the number and composition of heat intercepts in a thermal insulation system. *Engineering and Optimization*, 2 (1):5–29, 2001.
- [17] National Institute of Standards and Technology (NIST). Material properties. <http://cryogenics.nist.gov/MPropsMAY/materialproperties.htm>, 2012. Cryogenic Technologies Group.
- [18] A. R. Shouman. Nonlinear heat transfer and temperature distribution through fins and electric filaments of arbitrary geometry with temperature-dependent properties and heat generation. Technical report, NASA, Jan 1968.
- [19] Chi K. Tsao. Temperature distribution and power loss of a gas-cooled support for a cryogenic container. *Cryogenics*, 1974.

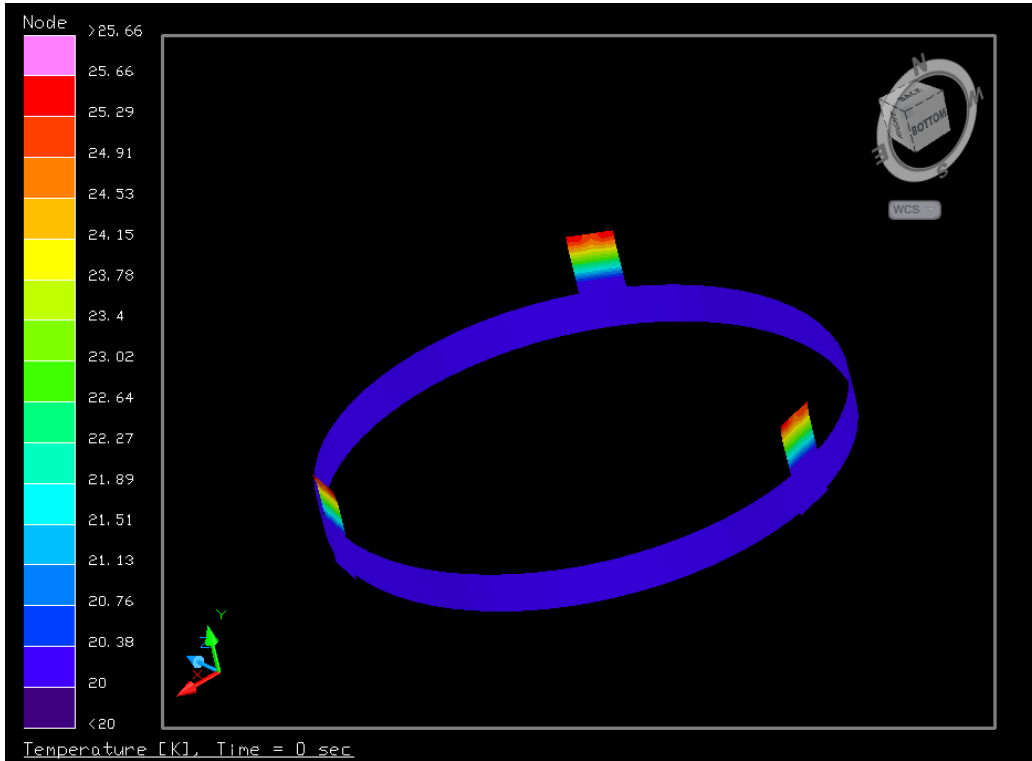


Figure 5: This is a picture of a thermal model of the Cryogenic Boil off Reduction System test. Most of the tank is ‘cut away’ for easier viewing, except for a central band, around which three ‘ear’ attachments create the mounting interfact between the tank and the support struts. The practicing engineer should expect a change in temperature across this attachment fixture, as shown in the screen capture. (*A ‘Cryogenic Boil off Reduction System’ thermal model by J.P. Elchert*)

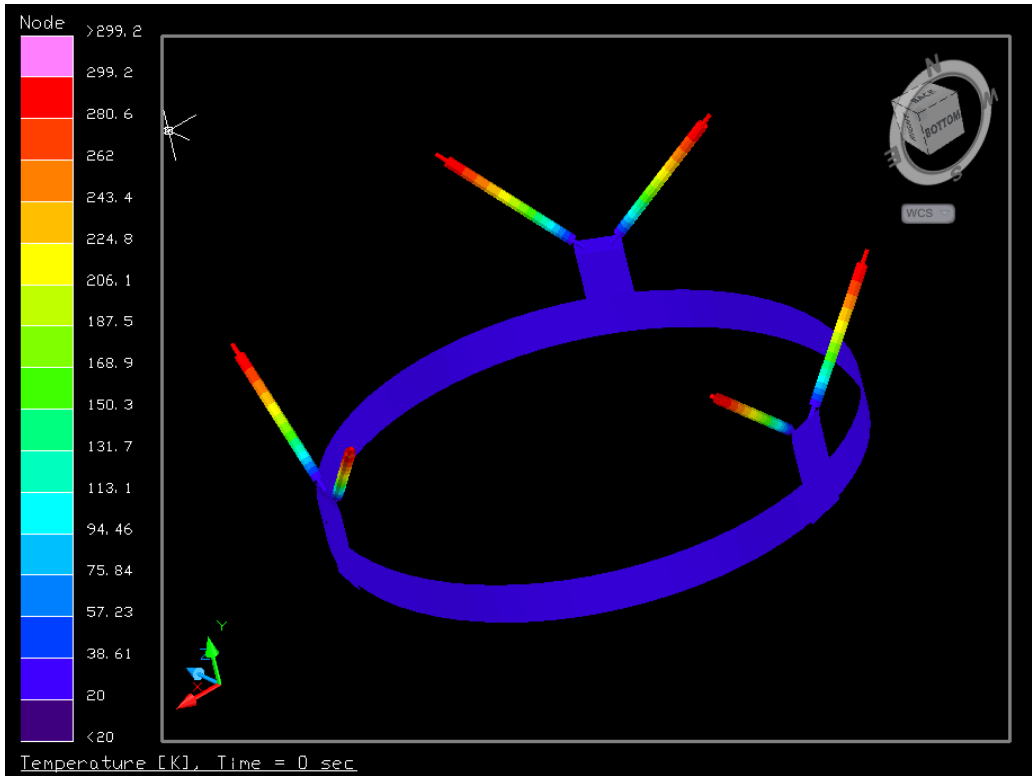


Figure 6: This is the same model shown in the previous figure, except this time the emphasis is on the struts. The strut provides excellent thermal isolation by utilizing a minimized area to length ratio, proper application of blankets or surface coating, and the best material. When considering all of these parameters, be sure to test several different materials because some are inherently better than others. (A 'Cryogenic Boil off Reduction System' thermal model by J.P. Elchert)

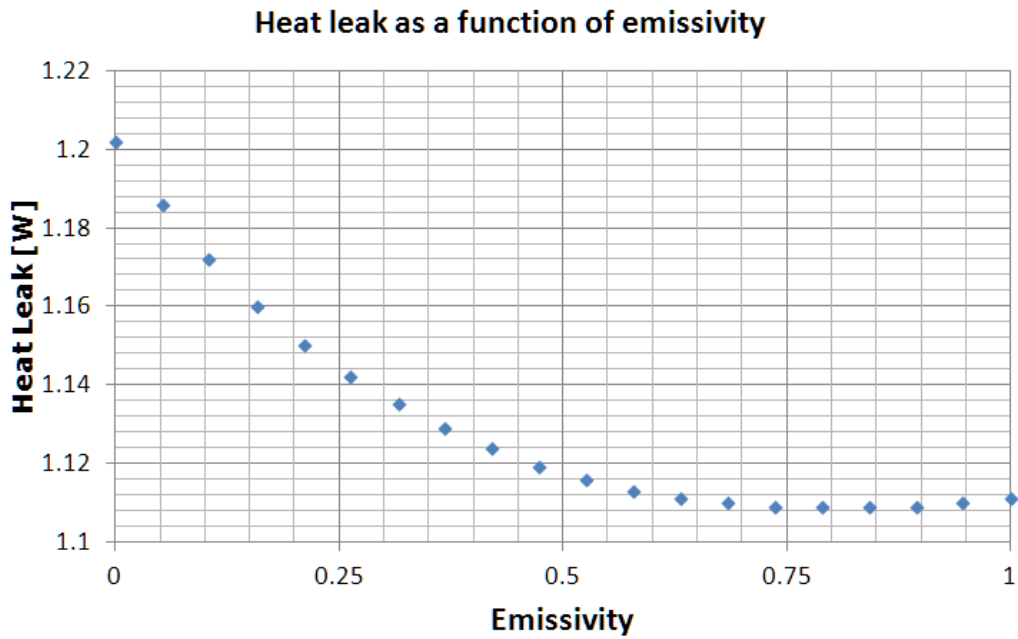


Figure 7: In this case, the hot boundary was 300K and the cold boundary was 20K. The large, isothermal surroundings temperature was 150K. Keep in mind that whether an optimum actually appears is also a function of the surroundings temperature. For example, if the surroundings temperature was 200K, the heat leak increases monotonically as a function of emissivity thus the optimum external emissivity is 0. Perfectly insulated from thermal radiation would be best for that case.

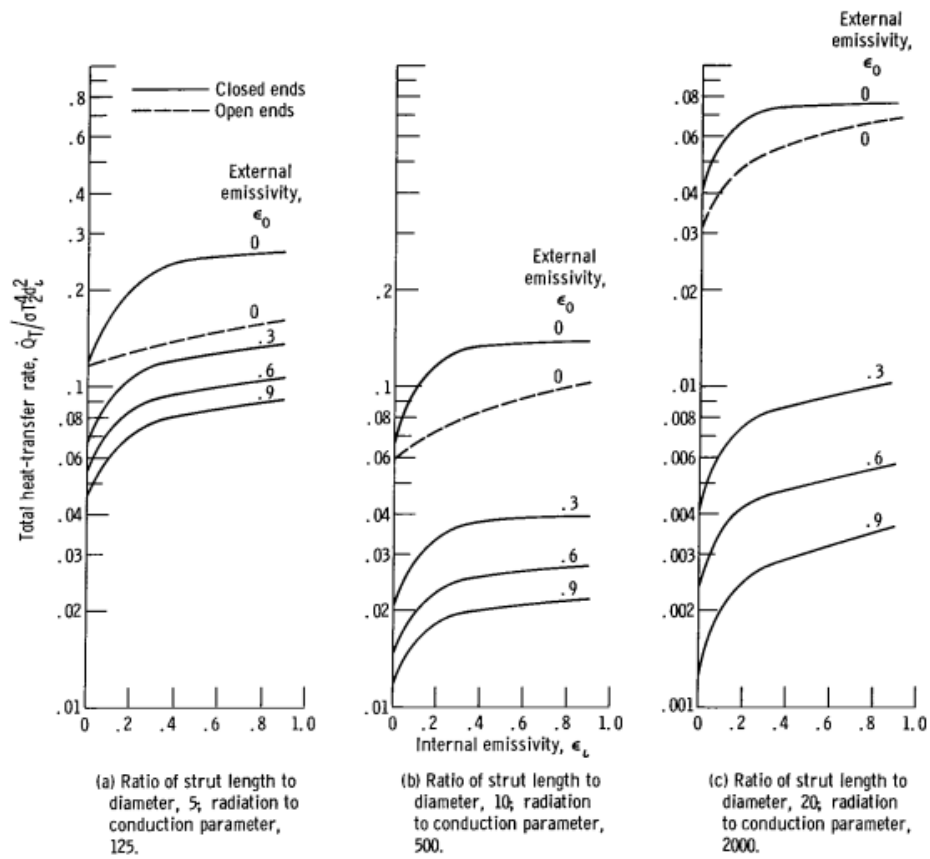


Figure 26. - Total heat-transfer rate through strut as function of internal and external emissivity.

Figure 8: In Boyle and Knoll's analysis, the external, large, isothermal surroundings temperature was taken to be 0K.

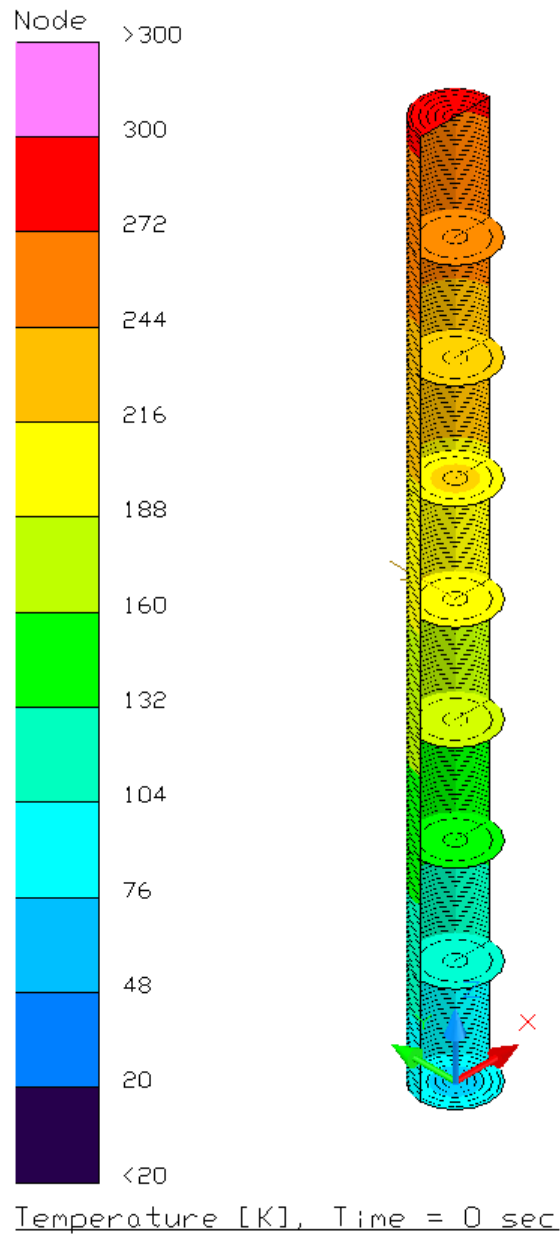


Figure 9: This is an example of a solved seven shield case. I always spaced shields equally, although I suspect a variable spacing is optimal. But that problem isn't terribly important to solve because the magnitude of the internal radiation effect is roughly 1% of the total heat transfer. I should point out that in composite tubes, the magnitude of internal radiation heat rate is roughly 5% due to radiation heat transfer being a bit more dominant for low conductivity materials.

Comparison of hypothetical configurations as a function of internal emissivity

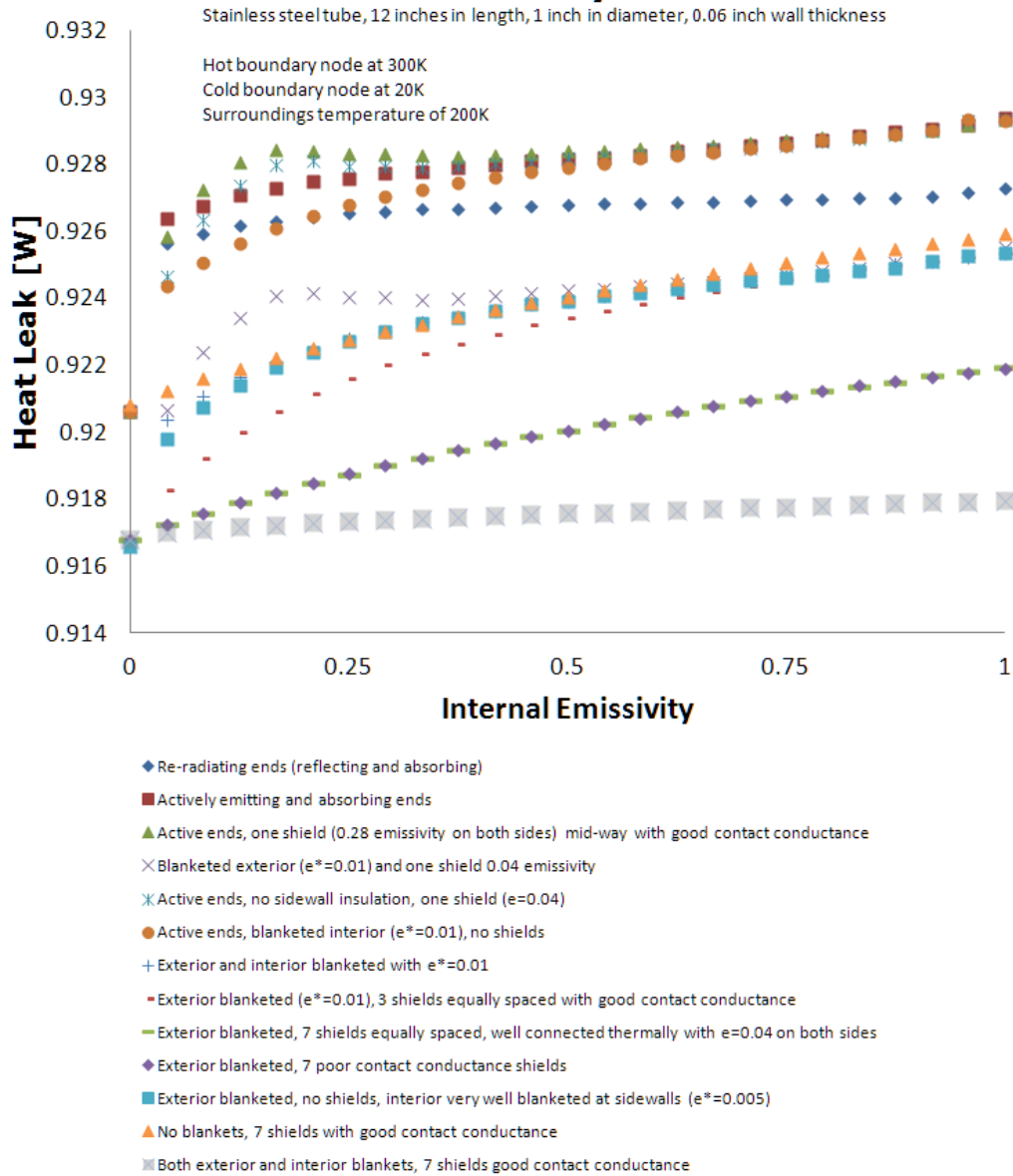


Figure 10: For the colorblind, the third series from the top of the legend (green triangles) has a peak magnitude of roughly 0.928W. Series 2 (red squares) also peaks around this number; series 1 (blue diamonds) peaks around 0.926W. For a detailed description of these curves, please see sub-section 4.2. 36

**In a radiation dominated environment,
increasing the length beyond a point yeilds
no additional reduction in heat flow**

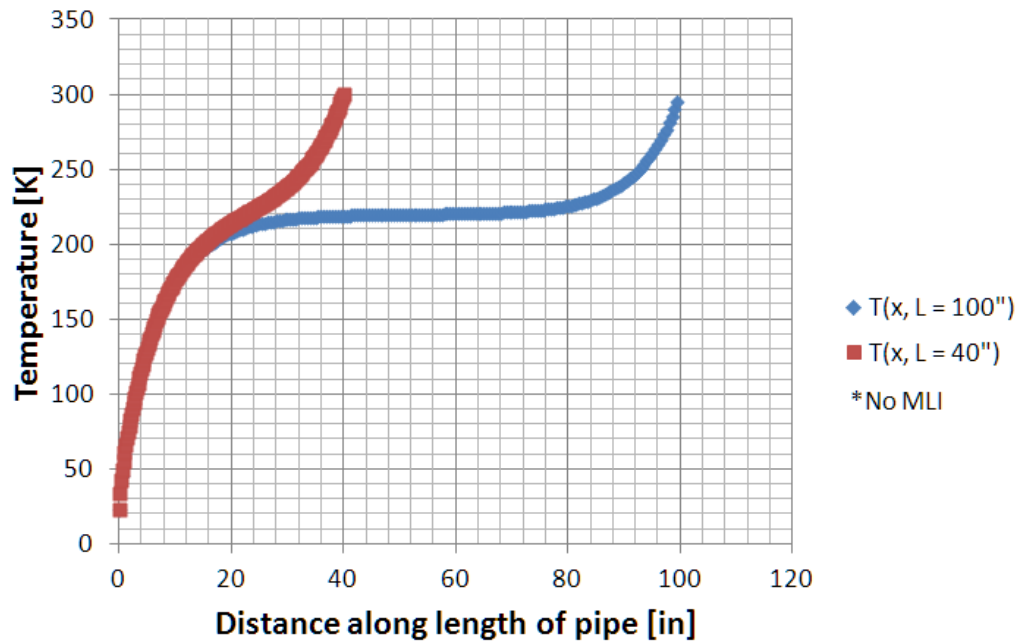


Figure 11: In this particular case, the tube had a high emissivity on the external surface, making it sensitive to the 220K boundary. That nonlinearity results in both tubes having roughly the same net heat leak into the cold boundary node—even though one is over twice as long. This illustrates the problem with using simple one-dimensional, linear analogies in a nonlinear domain. As soon as temperature dependent properties and thermal radiation enters the picture, the problem becomes strongly nonlinear, making any simple model useless for detailed design.

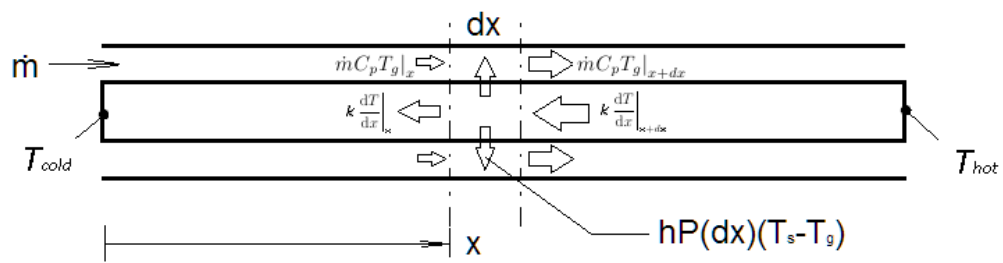


Figure 12: We are restricted to constant properties with no radiation for the analytical solution of the boil off problem.

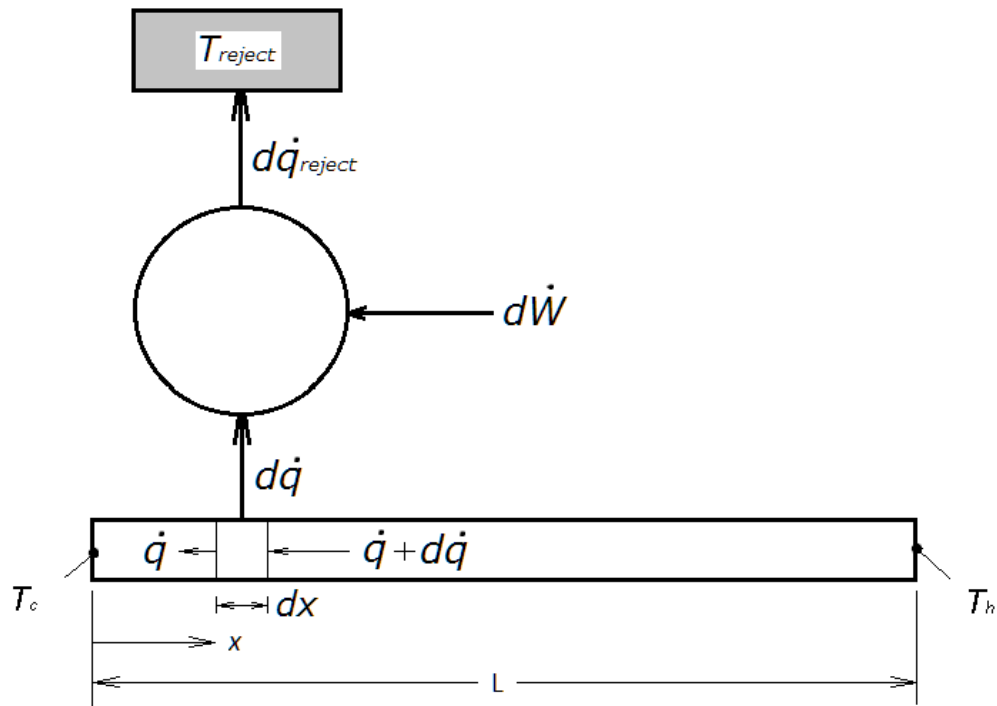


Figure 13: This figure depicts the abstract idea of infinitesimal refrigeration cycles continuously cooling every point along the strut. Bejan solved[3] this classical minimization problem, discovering the lowest possible bound for the total required refrigeration input power by hypothesizing continuous, differential, ideal, reversible Carnot cycles with perfect heat transfer. In a real application, the heat transfer area, attachment method, and contact resistance would result in the need for more heat removal than predicted. Nevertheless, this classic solution—now nearly 40 years old—was a valuable contribution to cryogenics research.

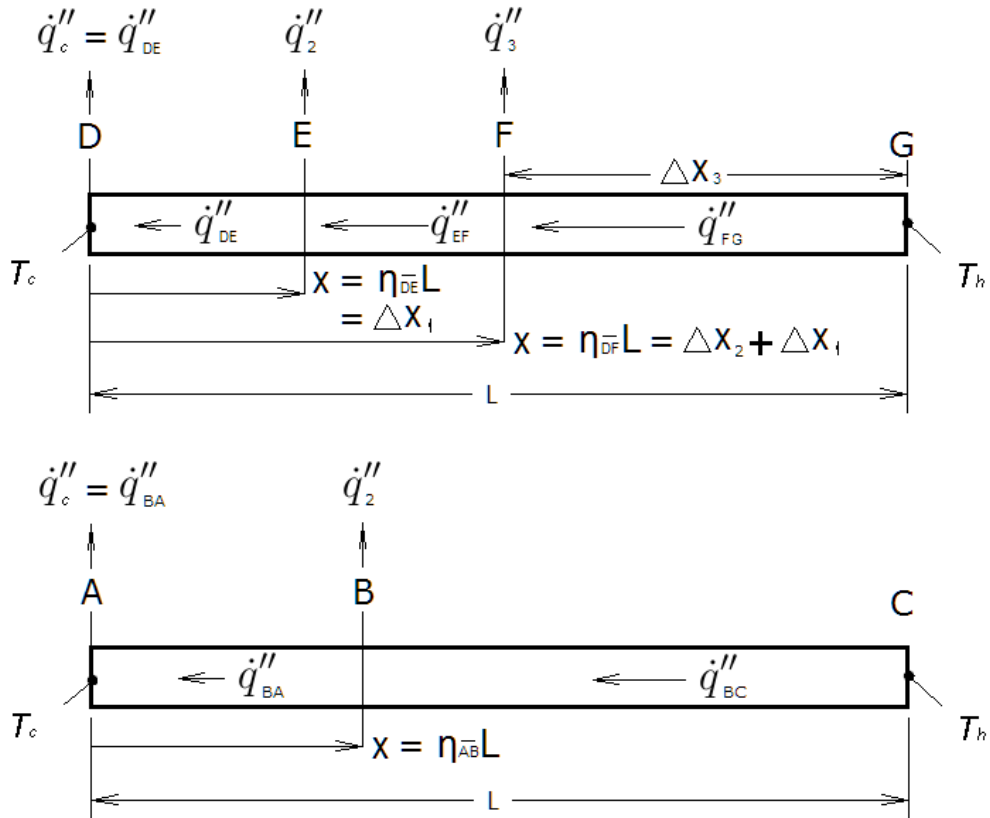


Figure 14: The lower drawing depicts two stage cooling whereas the upper drawing shows three stage cooling. In my formulation, all stages are measured from the cold end ($\eta_{\overline{AB}}$, for example). Notice that in Hilal and Boom's formulation, only the distance between stages is measured ($\Delta x_1/L$, $\Delta x_2/L$, or $\Delta x_3/L$).

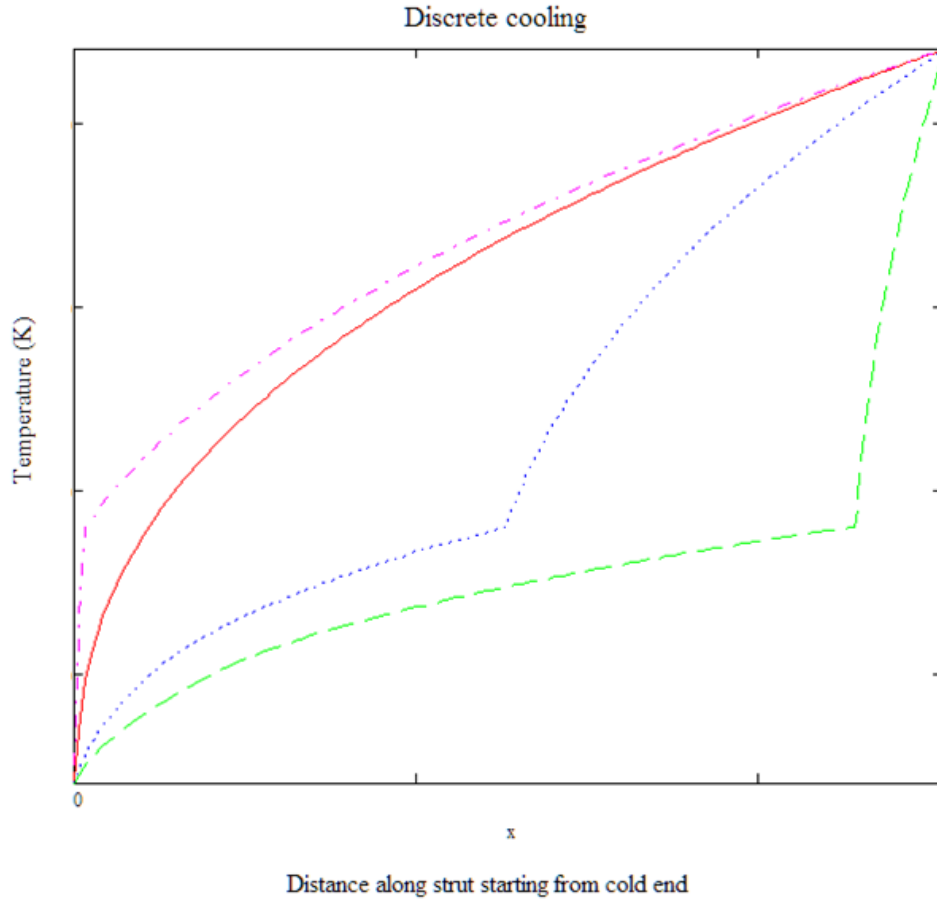


Figure 15: This figure depicts various ideal temperature profiles of a strut. The solid line shows the conduction only solution (no discrete cooling). The other lines show cooling at various locations on the strut, each at the same temperature. Observe that the effect of cooling is to decrease the temperature gradient at the cold end and increase the gradient at the warm end. The dash-dotted line actually shows a case where the coldest boundary is being warmed by the intercept. In that case, the intercept was located closer to the cold boundary than where the strut would naturally equal the intercept's temperature with no cooling at all. Here, the situation is reversed: the gradient at the cold end increased while the gradient at the hot end decreased.

Table II. Optimum Temperatures, Locations, and Refrigeration Power for Finite Number of Shields

Number of shields	Cycle*	T_1, K	T_2, K	T_3, K	$\Delta x_1/L$	$\Delta x_2/L$	$\Delta x_3/L$	$\Delta x_4/L$	$PL/A, W/cm$
304 Stainless steel ($T_c = 4.2 K$)									
1	C	39.7	—	—	0.338	0.662	—	—	445
1	A	39.7	—	—	0.338	0.662	—	—	1781
2	C	21.6	81.7	—	0.189	0.334	0.477	—	316

* C, Carnot cycle efficiencies; A, actual cycle efficiencies.

Figure 16: The covered discrete, two stage optimization example problem matches Hilal and Boom’s 1977 solution[12] to the same problem. Note that when comparing formulations, T_c goes unlisted in Hilal’s table, and $T_{2\text{Elchert}} = T_{1\text{Hilal}}$ and $T_{3\text{Elchert}} = T_{2\text{Hilal}}$. Also, note that Hilal does not explicitly show $\eta_{\overline{DF}}$ in the table, instead representing it indirectly with $\Delta x_1/L + \Delta x_2/L$. This can be a bit confusing for folks who mistakenly assume $\Delta x_2/L \equiv \eta_{\overline{DF}}$, which is false. Also, Hilal and Boom went further by including a real coefficient of performance (A, ‘actual cycle efficiencies used’). Unfortunately, there’s a typographical error in their table. Observe the first and second rows. The second row matches the first row (except for the [Watts/(area-to-length ratio)]).

In my estimate, the second row is actually correct. Because solving the Carnot case gives $T_2 = 40K$ and $\eta_{\overline{AB}} = 0.351$ and when I tested a sample real coefficient of performance, I found roughly $T_2 = 39K$ and $\eta_{\overline{AB}} = 0.33$. So the first row—the Carnot case—was misprinted. Hilal and Boom actually had solutions up to four stages and also studied the same solutions for Narmco 570 cloth, but that information, being irrelevant, was omitted.

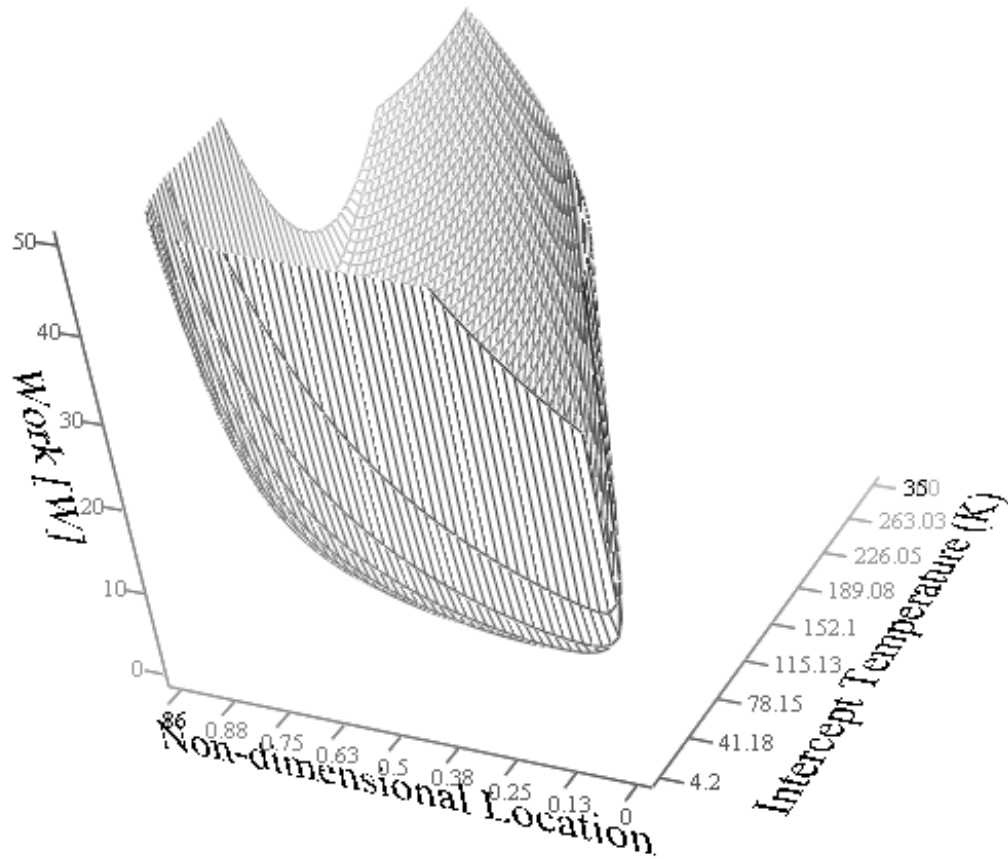


Figure 17: The surface represents, graphically, how the required refrigeration work changes with the location and temperature of the intercept stage (two stage, Carnot example with 100 cm stainless steel 304). Surprisingly, because of the hull-shaped surface, there exists a locus of points in the domain giving roughly the same value in the range. Note that the nondimensional location in the Figure is equivalent to η_{AB} in the text.